

# Demodulation of a single-image interferogram using a Zernike-polynomial-based phase-fitting technique with a differential evolution algorithm

Chao Tian, Yongying Yang,\* Tao Wei, Tong Ling, and Yongmo Zhuo

State Key Laboratory of Modern Optical Instrumentation, Zhejiang University, 38 Zheda Road, Hangzhou 310027, China

\*Corresponding author: chuyyy@zju.edu.cn

Received April 19, 2011; revised May 12, 2011; accepted May 18, 2011;  
posted May 18, 2011 (Doc. ID 146267); published June 14, 2011

We propose a simple and robust polynomial-based phase-fitting (PPF) technique for single interferogram demodulation. Based on the smoothness assumption, the method employs a set of Zernike polynomials (ZPs) to fit the phase and estimates the expansion coefficients using a global optimization algorithm, i.e., differential evolution. The fitting order of the ZPs and the bounds of the coefficients can be intuitively determined according to the shape and number of fringes of the interferogram. Different from classical methods that need predefined scanning paths to guide the phase estimator, the PPF demodulates an interferogram globally and is insensitive to local defects, which allows it to deal with very noisy interferograms. Moreover, as the PPF gives the reconstructed phase by use of the ZPs, no further phase-unwrapping or wavefront-fitting procedures are needed. Experimental results have demonstrated the robustness and effectiveness of the method. © 2011 Optical Society of America

OCIS codes: 100.2650, 100.5070, 120.3180, 120.5050.

Phase extraction from a single interferogram is important for successful applications of optical interferometry to the measurement of a wide range of physical quantities [1], which, however, is a difficult task. In the past few years, many algorithms have been proposed to solve this problem, such as regularized phase tracing (RPT) [2–4], spiral phase quadrature transform [5], and frequency-guided sequential demodulation [6]. In this Letter, we present a simple and robust polynomial-based phase-fitting (PPF) technique that is capable of demodulating single open- or closed-fringe interferograms.

Generally, a fringe pattern  $I(x, y)$  can be formulated as

$$I(x, y) = a(x, y) + b(x, y) \cos[\phi(x, y)] + n(x, y), \quad (1)$$

where  $a(x, y)$  and  $b(x, y)$  are the background and modulation terms, respectively,  $\phi(x, y)$  is the phase to be recovered, and  $n(x, y)$  is the additional noise. After normalization [7], Eq. (1) may be simplified as

$$I_n(x, y) = \cos[\phi(x, y)], \quad (2)$$

where  $I_n(x, y)$  is the normalized intensity. Assuming that the phase  $\phi(x, y)$  to be recovered is continuous, we may find an approximation function  $\tilde{\phi}(x, y)$  of it, which can be written as a linear combination of  $N$  terms of independent polynomials up to an order  $n$ ; that is,

$$\phi(x, y) \cong \tilde{\phi}(x, y) = \tilde{\phi}(\mathbf{c}; x, y) = \sum_{i=1}^N c_i \psi_i(x, y), \quad (3)$$

where  $\mathbf{c}$  are the expansion coefficients of the basis functions  $\psi_i(x, y)$  whose maximum order is no greater than  $n$ . Since the Zernike polynomials (ZPs) [8] are related to classical aberrations in optics, we choose them against many others, such as the power polynomials and the Chebyshev polynomials. Note that, as the ZPs are defined on a unit disk, the pupil of the interferogram is restricted to be circular. When written in polar coordinates, the nonnormalized ZPs are given by

$$\left. \begin{aligned} \psi_{\text{even}i} &= R_n^m(\rho) \cos m\theta \\ \psi_{\text{odd}i} &= R_n^m(\rho) \sin m\theta \\ \psi_i &= R_n^m(\rho) \end{aligned} \right\} \begin{array}{l} m \neq 0 \\ m = 0 \end{array}, \quad (4)$$

where  $i$  is a mode ordering number and

$$R_n^m(\rho) = \sum_{s=0}^{(n-m)/2} \frac{(-1)^s (n-s)! \rho^{n-2s}}{s! [(n+m)/2 - s]! [(n-m)/2 - s]!}, \quad (5)$$

where the indices  $n$  and  $m$  are radial degree and the azimuthal frequency, respectively, and satisfy  $m \leq n$ ,  $n - |m| = \text{even}$ . The relation between  $N$  and  $n$  is  $N = (n+1)(n+2)/2$ . By using Eqs. (2) and (3), we get

$$I_n(x, y) \cong \cos[\tilde{\phi}(\mathbf{c}; x, y)]. \quad (6)$$

To estimate the expansion coefficients  $\mathbf{c}$ , we should try to minimize the cost function:

$$f(\mathbf{c}) = \sum_{(x,y) \in L} (\{I_n(x, y) - \cos[\tilde{\phi}(\mathbf{c}; x, y)]\}^2 + \lambda I_n^2(x, y) [1 - \gamma_n(\mathbf{c})]), \quad (7)$$

where  $L$  is a two-dimensional aperture,  $\lambda$  is a constraint parameter, and  $\gamma_n$  is a normalized correlation coefficient that measures the similarity between the estimated interferogram and the real one, which is defined as

$$\gamma_n(\mathbf{c}) = \frac{\left\{ \sum_{(x,y) \in L} I_n(x, y) \cos[\tilde{\phi}(\mathbf{c}; x, y)] \right\}^2}{\left[ \sum_{(x,y) \in L} I_n^2(x, y) \right] \left[ \sum_{(x,y) \in L} \cos^2[\tilde{\phi}(\mathbf{c}; x, y)] \right]}. \quad (8)$$

To demodulate the fringe pattern in Eq. (2), we use a differential evolution (DE) algorithm [9] to find the global minimum of the multimodal cost function.

The DE algorithm, which is a powerful population-based stochastic search technique for multidimensional optimization, works with a population of  $N \times NP$  dimensional parameter vectors (i.e., individuals)  $\mathbf{C}_j^G =$

$[c_{1,j}^G, c_{2,j}^G, \dots, c_{N,j}^G]^T, j = 1, 2, \dots, NP$  and aims at evolving it toward the global minimum iteratively by three steps, i.e., the mutation, the crossover, and the selection. Defining the upper and lower bounds of the search ranges as  $UB = [c_{1\max}, c_{2\max}, \dots, c_{N\max}]^T$  and  $LB = [c_{1\min}, c_{2\min}, \dots, c_{N\min}]^T$ , the original population can be initialized by

$$c_{i,j}^0 = c_{i\min} + \text{rand}(0, 1) \times (c_{i\max} - c_{i\min}), \quad (9)$$

where  $i = 1, 2, \dots, N$ ,  $c_{i,j}^0$  is the  $i$ th parameter in the  $j$ th individual at the zeroth generation and  $\text{rand}(0, 1)$  represents a uniformly distributed random variable within  $[0, 1]$ .

After the initialization, we use a mutation strategy [9], i.e., DE/rand/1/bin to yield a mutant vector  $\mathbf{V}_j^G = [v_{1,j}^G, v_{2,j}^G, \dots, v_{N,j}^G]^T$  with respect to  $\mathbf{C}_j^G$  according to

$$\mathbf{V}_j^G = \mathbf{C}_{r_1}^G + F(\mathbf{C}_{r_2}^G - \mathbf{C}_{r_3}^G), \quad (10)$$

where  $r_1, r_2, r_3 \in [1, 2, \dots, NP]$  are three random integer indices different from the running index  $j$  and satisfy  $r_1 \neq r_2 \neq r_3$ , and  $F \in [0, 2]$  is a factor that controls the amplification of the differential variation  $(\mathbf{C}_{r_2}^G - \mathbf{C}_{r_3}^G)$ .

Then we generate a trial vector  $\mathbf{U}_j^G = [u_{1,j}^G, u_{2,j}^G, \dots, u_{N,j}^G]^T$  by the crossover of  $\mathbf{C}_j^G$  and  $\mathbf{V}_j^G$  according to

$$u_{i,j}^G = \begin{cases} v_{i,j}^G, & \text{if } \text{rand}_i(0, 1) \leq \text{CR} \text{ or } i = i_{\text{rand}} \\ c_{i,j}^G, & \text{otherwise} \end{cases}, \quad (11)$$

where CR is a user-defined crossover constant within the range  $[0, 1]$ ,  $\text{rand}_i(0, 1)$  is a random number for the  $i$ th parameter, and  $i_{\text{rand}}$  is a uniformly distributed random integer within the range  $[1, N]$ . Here, if the values of  $\mathbf{U}_j^G$  exceed the corresponding bounds, we may randomly reinitialize them to keep their values within the bounds.

Finally, a greedy criterion that is described as

$$\mathbf{C}_j^{G+1} = \begin{cases} \mathbf{U}_j^G, & \text{if } f(\mathbf{U}_j^G) \leq f(\mathbf{C}_j^G) \\ \mathbf{C}_j^G, & \text{otherwise} \end{cases}, \quad (12)$$

can be used to decide whether the trial vector  $\mathbf{U}_j^G$  should become a member of the generation  $G + 1$ .

Repeat the three steps above until the user-defined termination criteria are satisfied.

Once the expansion coefficients  $\mathbf{c}$  are estimated by the DE, they may be substituted back into Eq. (3) to yield an estimate of the true phase.

In the PPF system, two factors, that is, the fitting order  $n$  and the bounds of the expansion coefficients  $\mathbf{c}$  are critical to the success and the convergence of the demodulation. For a given interferogram, the fitting order  $n$  can be determined according to the complexity of the shape of the interferogram as well as the Seidel aberrations (see [1] for details) in it. For example, if an interferogram has some dominant aberrations, the fitting order  $n$  should not be smaller than the orders of ZPs that contain these components. In the experiments presented, the values of  $n$  we used ranged from 2 to 8.

In addition, the bounds of the expansion coefficients  $\mathbf{c}$  can be determined according to the number of fringes in the entire or partial interferogram. Specifically, if an in-

terferogram has  $p$  fringes, the bounds can be obtained by simply setting  $c_{i\max} = -c_{i\min} = p\pi$  because the values of the nonnormalized ZPs [Eq. (4)] are all within the range  $[-1, 1]$  [i.e.,  $\phi(\mathbf{c}; x, y) \in [-1, 1]p\pi$ ]. The rule has a universal significance and can be applied to all situations. However, we may practically optimize the bounds further due to the following two facts: (1) the phase is often governed by some classical aberrations that are related to the ZPs and (2) the coefficients gradually become smaller with the increase of the order of the ZPs. Therefore, the bounds can be written in a more practical way; that is,

$$\begin{aligned} UB &= [1, \alpha_1 \text{ones}(1, 2), \dots, \alpha_n \text{ones}(1, n+1)]^T \pi, \\ LB &= [-1, 0, \alpha_1, \dots, \alpha_n \text{ones}(1, n+1)]^T \pi, \end{aligned} \quad (13)$$

where  $0 \leq \alpha_1, \alpha_2, \dots, \alpha_n \leq p$  are weight coefficients and  $\text{ones}(1, n+1)$  is a  $1 \times (n+1)$  unit vector. In this way, we may choose different values of  $\alpha_n$  to control the bounds for different situations. Note that the ranges of  $c_1$  and  $c_2$  are set to  $[-1, 1]\pi$  and  $[0, \alpha_1]\pi$  due to the periodic and even properties of the cosine function.

For fringe patterns, such as moiré or photoelastic ones, that probably do not have obvious components related to the aberrations, it may be difficult to use the rules above to determine the fitting order and the bounds. This is also true for interferograms with square apertures when the Chebyshev or Legendre polynomials are used. In these cases, we have to empirically try different values of  $n$  and  $\alpha$  and choose a better combination. Besides, as the computation time increases rapidly with the growth of  $n$ , the proposed PPF may be inappropriate to occasions such as speckle metrology and photoelasticity where fringe patterns may have high spatial frequency content or very irregular shapes if no masks are defined.

To verify the performance of the PPF, we tested it through three experiments, in all of which we used  $\lambda = 1$ ,  $NP = 10N$ ,  $CR = 1$ , and  $F = 0.5[1 + \text{rand}(0, 1)]$  based on a computer with Core 2 Duo CPU of 2.1 GHz main frequency using MATLAB.

We first carried out an experiment to compare the demodulation results by the PPF and the RPT. Figures 1(a) and 1(b) show an experimental interferogram with  $128 \times 128$  pixels and its normalized intensity [7], respectively. We demodulated the fringe pattern by the RPT with a neighborhood  $N_{xy} = 7$  and a phase shift  $\alpha = 0.2\pi$  rad, as well as the PPF with a fitting order  $n = 2$ , and showed their correspondingly demodulated phase and their cosine values in Figs. 1(c), 1(e), 1(d), and 1(f). In the PPF, the weight coefficients of the bounds are set to  $\alpha_1 = \alpha_2 = 7$  because the maximum number of fringes in the interferogram is 7. The normalized similarity  $\gamma_n$  [Eq. (8)] between Figs. 1(d) and 1(f) and Fig. 1(b) are 0.419 and 0.680, respectively. The total time used by the RPT and the PPF is 124 and 29 s, respectively.

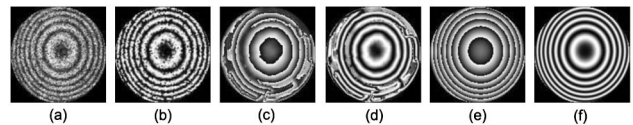


Fig. 1. Demodulation results by the RPT and the PPF.

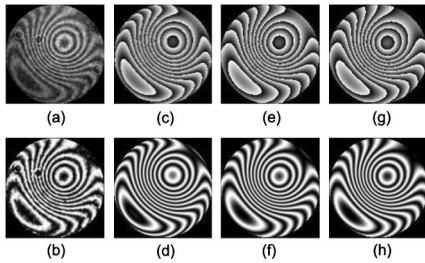


Fig. 2. Demodulation of a real interferogram using the PPF.

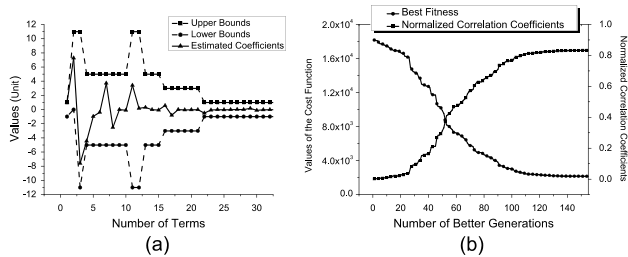


Fig. 3. Demodulation results of Fig. 2(g).

Figure 2 shows a  $128 \times 128$  pixel real interferogram [Fig. 2(a)] that was successfully demodulated by the PPF. Figure 2(b) is the normalized intensity. Figures 2(c), 2(e), 2(g), 2(d), 2(f), and 2(h) are the recovered phase by use of the 5, 6, and 7 orders of the ZPs, respectively, and their corresponding cosine values. The calculated  $\gamma_n$  between Figs. 2(d), 2(f), and 2(h) and Fig. 2(b) are 0.585, 0.814, and 0.834, respectively. As we can see, the reconstructed phase in Fig. 2(c) has some edge distortions due to lack of fit and these distortions almost disappear in Figs. 2(e) and 2(g), which indicates that the fitting order  $n$  should be preferably larger than 5. Since large tilt and spherical aberration components [1] are present in the interferogram, the preassigned bounds are  $UB = [1, 11, 11, 5, 5, 5, 5, 5, 5, 5, 11, 11, 5, 5, 5, 3 \times \text{ones}(1, 6), 1 \times \text{ones}(1, 15)]^T \pi$  and  $LB = [1, 0, 11, 5, 5, 5, 5, 5, 5, 5, 11, 11, 5, 5, 5, 3 \times \text{ones}(1, 6), 1 \times \text{ones}(1, 15)]^T \pi$ , respectively, which, along with the estimated coefficients  $\mathbf{c}$  of the phase in Fig. 2(e), are shown in Fig. 3(a). Figure 3(b) shows the changes of the best fitness and the  $\gamma_n$  for Fig. 2(g). Note that the data given here are typical from many experiments.

Finally, Fig. 4 shows another interferogram [Fig. 4(a)] with  $256 \times 256$  pixels that was successfully demodulated by the PPF. The normalized irradiance is shown in Fig. 4(b). Figures 4(c), 4(e), 4(g), 4(d), 4(f), and 4(h) are the recovered phase by use of 6, 7, and 8 orders of the ZPs, respectively, and their corresponding cosine values. The corresponding  $\gamma_n$  are 0.770, 0.848, and 0.861. The weights of the bounds are set to  $\alpha_1 = 12$ ,  $\alpha_2 = \alpha_3 = 10$ ,  $\alpha_4 = 4$ ,  $\alpha_5 = 2$ , and  $\alpha_6 = \alpha_7 = \alpha_8 = 1$ . The DE used 5042, 11,345, and 28,975 s to evolve 3302, 4577, and 8359 generations to search the optimal solutions for the three fitting orders. To see how time consuming the PPF is, we also sampled Fig. 4(a) by  $512 \times 512$  pixels and repeated the demodulation process with  $n = 8$ . The PPF used about 36 h to give the best phase map, which is quite a

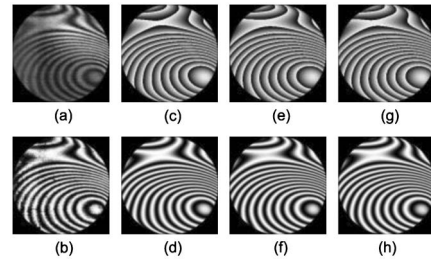


Fig. 4. Demodulation of a complex interferogram.

long time compared with the method by Dalmau-Cedeño *et al.* in [10], where the authors claim an inferior demodulation time (about 9 s for a  $512 \times 512$  pixels fringe pattern). The main reasons are that we use a global search algorithm here and Dalmau-Cedeño *et al.* take advantage of fast algorithms widely used for open fringe patterns. Note that the computation time here can be reasonably reduced by properly adjusting the parameters, such as  $n$ , UB, LB,  $NP$ ,  $F$ , and CR.

In conclusion, we propose a simple and robust PPF technique for single interferogram demodulation. As the fit and the optimization are done in a global sense, the PPF is a global phase demodulator in nature, which makes it quite robust to noise (Figs. 1, 2, and 4). It is due to this nature that the PPF may give inaccurate results for phase maps that are not well defined locally, such as defects and discontinuities. For these cases, masks may be defined to avoid these subregions. The reader must be aware that, as the ZPs are not orthogonal for apertures other than a unit disk, the expansion coefficients will become dependent on each other and be affected by the values of the fitting order  $n$ . Although the demodulation of a complex interferogram using the PPF requires a huge amount of computation due to the global search, this problem may be ultimately solved with the developments of parallel computation and graphics processing units.

Thanks to the referees for their insightful comments. This work was supported by the Aerospace Innovation Fund of the China Aerospace Science and Technology Corporation (CASC) under grant 2009200054.

## References

1. D. Malacara, *Optical Shop Testing* 3rd ed. (Wiley, 2007).
2. M. Servin, J. L. Marroquin, and F. J. Cuevas, *Appl. Opt.* **36**, 4540 (1997).
3. J. L. Marroquin, R. Rodriguez-Vera, and M. Servin, *J. Opt. Soc. Am. A* **15**, 1536 (1998).
4. C. Tian, Y. Yang, S. Zhang, D. Liu, Y. Luo, and Y. Zhuo, *Opt. Lett.* **35**, 1837 (2010).
5. K. G. Larkin, D. J. Bone, and M. A. Oldfield, *J. Opt. Soc. Am. A* **18**, 1862 (2001).
6. Q. Kemao and S. H. Soon, *Opt. Lett.* **32**, 127 (2007).
7. J. A. Quiroga, J. A. Gomez-Pedrero, and A. Garcia-Botella, *Opt. Commun.* **197**, 43 (2001).
8. R. J. Noll, *J. Opt. Soc. Am.* **66**, 207 (1976).
9. R. Storn and K. Price, *J. Global Optim.* **11**, 341 (1997).
10. O. S. Dalmau-Cedeño, M. Rivera, and R. Legarda-Saenz, *J. Opt. Soc. Am. A* **25**, 1361 (2008).